


Investigation of Novel, Internally Hollowed Structured Stainless Steel to Reduce Stress Shielding

Mohammadreza Yazdifar^{1*} 

Ebrahim Esat² 

Mahshid Yazdi Far¹ 

¹ School of Mechanical Automotive Aerospace, Coventry University, UK

² School of Mechanical, Design and Physical Science, Brunel University, UK

ABSTRACT

There are many aspects that have direct effects on total hip replacement performance (THR), such as material properties, applied loads, surgical approach, femur size and quality, prosthesis design, bone-implant interface etc. One of the purposes to study different structure in THR is reducing the stress shielding. For the current study, an innovative hollow spherical structure is developed for femoral hip stems. The aim is to extract volume in the spherical shape from the stainless-steel hip implant stems, in order to focus solely on correlating with titanium behaviour. Internal geometry for the femoral stem is optimised in order to transfer more stress onto the bone. Moreover, the approach involves extracting volume in the spherical shape from internal structure to reduce stress shielding. New novel implant is proposed that demonstrated reduction in stress shielding. The sphered models have a smaller young's modulus and strength than the solid stainless-steel sample. The spheres in hollowed structures reduce the stress shielding and they transfer more stress onto the bone when compared to the solid stainless-steel models. This approach also involves restructuring a hard material, such as stainless steel, to enhance osseointegration. The reduction of the young's modulus and stress directly depends on the volume of the hollow spheres in the models; however, there is certain volume that can be extracted from solid.

Keyword: Structured Stainless Steel, Reduce Stress Shielding

©2021 The Authors. Published by Fundamental Journals. This is an open-access article under the CC BY-NC
<https://creativecommons.org/licenses/by-nc/4.0/>

INTRODUCTION

The current materials used in biomedical engineering cannot compete with the material properties of bone [1]. The main biomedical metals used for medical applications are stainless steel, Co alloys and Ti alloys [2, 3]. One of the most important failure aspects that all implants face is stress shielding. The higher the rigidity

of the implant, the more chance of getting bone resorption, as the implant will transfer a smaller amount of load to the bone [4]. If the stiffness of an implant decreases, an increase in load transfer from the femoral stem to the proximal femur will occur, which results in decreasing of the stress shielding [5].

The elastic modulus of femoral stems is usually higher (e.g. Cobalt Chromium is 100 GPa) than the cortical bone (20.3 GPa) [4].

Stress shielding will increase if the rigidity of femoral stem increases. Which will result in bone density reduction in the proximal femur.

Jergesen and Karlen [6] looked at patient data covering large, medium and small stems. They found greater stress shielding in patients with large stems those with smaller ones. Nowadays, most of the stem designs are aimed at improving the load-transfer mechanism through the femur [6].

Researchers has been working on implant optimisation in order to reduce the stiffness of implants. Few studies focused on a hollowed implant [7] [8] [9] [10] [11] and reported reduction of stress shielding. Auxetic materials were introduced in 2014 for impact protector devices, such as pads, gloves, helmets and mats. These have a negative Poisson ratio or when they are under one directional force, they are thicker in one or more perpendicular directions [12].

Furthermore, honeycomb geometries were added to the stem design in new total hip replacement implants. These geometries were analysed using the finite element method and the auxetic stems showed a

reduction in the stress shielding effect [13]. Stress shielding is a major problem and that reducing Young's modulus could solve the issue. One of the ways to reduce the young modulus is to have a porous structure. These days with the help of 3D printing technique many porous structures have been developed for biomedical application [14] [15] [16] [17].

METHOD

To investigate the effect of stress shielding in hip implant for hollowed structure sets of FEA, experiments and mathematical model were designed. The spheres were created uniformly all over the samples and the results obtained from experiment, FEA and mathematical model showed the transfer of stress onto the bone. Comparing the hollowed structure with solid structure and also comparing the different geometries in the structure to evaluate which model reduce stress shielding in hip implant.

DESIGN

The height used to design small specimen for hollowed light weight material were obtained from the standard ASTM E9, 2000 for the metallic compression testing.

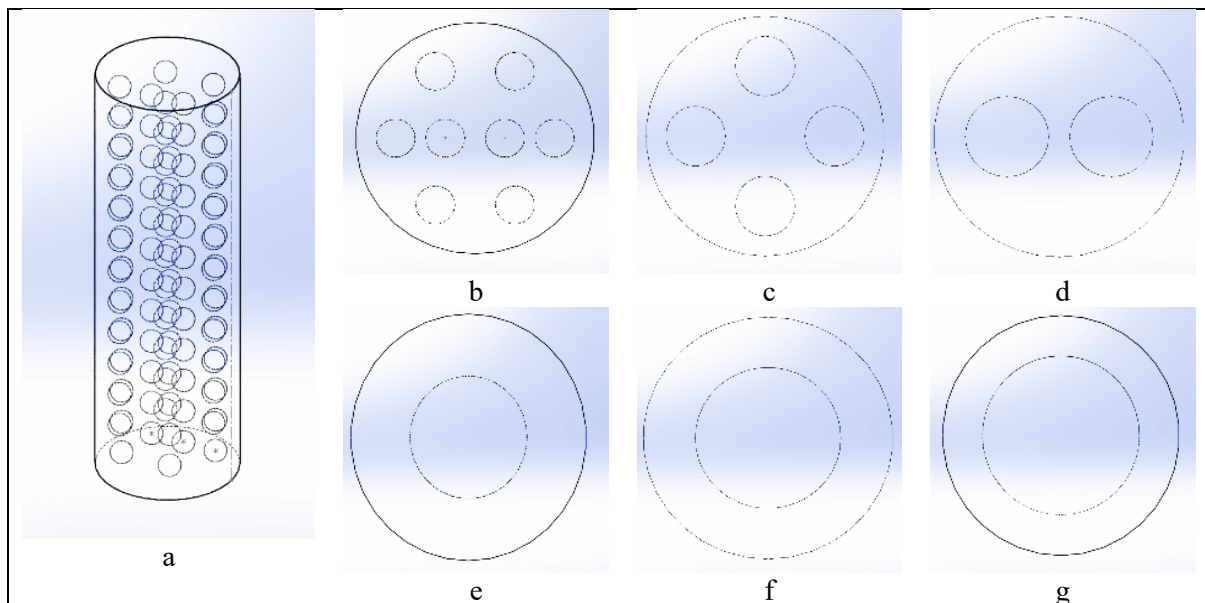


Figure 1: Uniformly distributed hollowed sphere along the metal with different diameter a) 1 mm 3D model view b) 1 mm c) 1.5 mm d) 2 mm e) 3 mm f) 3.5 mm g) 4 mm

Twelve different cylinders were designed in SolidWorks for stress analysis in order to see the difference in stress distribution over a constant volume. The spheres were created uniformly all over the samples and the results obtained showed the transfer of stress onto the bone. SolidWorks 2014 SP 4.0 was used to design the samples. Radius of hollowed spheres

change from 1 mm to 4 mm. This is to investigate of having hollow voids throughout the samples distributed uniformly, as shown in Figure 1, to reduce the Young's modulus. Reducing this, will reduce the stiffness of the materials and the less this is, the more deformation occurs and more stress is transferred to the surrounding area.

FINITE ELEMENT ANALYSIS

In this section, details about materials, meshing strategies, and the different loading conditions that were applied to the samples for analysis, are provided. FEA was used to analyse seven different porous cylindrical models. These differences pertained to the sphere sizes, their distance from wall surface and their distance from each other. In addition, the spheres were distributed evenly in these specimens to find out how they would affect the stress distribution over a controlled volume. SolidWorks 2014 SP 4.0 was used to model the parts and they were exported into FEA software for analysis. The aim of the numerical approach was to evaluate stiffness and stress on the outer surfaces through different internal structural

designs in a controlled volume. The boundary condition was made to make sure that it is aligned with experimental carried out.

EXPERIMENT

The compression test was also applied to the samples based on ASTM E9 and the rule of mixtures was used to measure Young's modulus and the strength of each sample. Samples weights were measured by scale to confirm the reduction in mass when containing hollow spheres. The height and diameter of the samples were also measured by a digital Vernier calliper to calculate their volume. Table displays the mass and dimensions of the samples.

Table 1: Weight and dimension of the samples measured by scale and a digital Vernier calliper

<i>Samples</i>	<i>Mass (g)</i>	<i>r (mm)</i>	<i>h (mm)</i>	<i>Vol (mm³)</i>
<i>R1.5</i>	34	6.1183	38.096	4480.132
<i>R1</i>	34	6.1283	38.116	4497.148
<i>R2</i>	34	6.126	38.116	4493.773
<i>R3</i>	33	6.1283	38.126	4498.328
<i>R3.5</i>	34	6.125	38.14	4495.135
<i>R4</i>	33.6	6.1316	38.143	4505.182
<i>Solid</i>	35	6.1316	38.126	4503.174

A compression test was applied to all the samples under the same conditions at room temperature.

Figure demonstrates one of the samples between the compression anvils. The stress-strain graphs were extracted from the tests for each sample. Furthermore, compression modulus and ultimate compression stress were obtained from the tests, the results of which were compiled in a stress-strain graph.

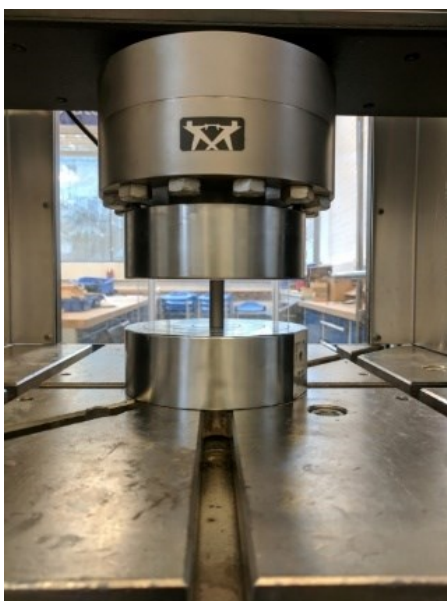


Figure 2: One of the samples between compression anvils

RULE OF MIXTURES

Various composite properties of composite materials can be predicted using a weighted mean technique known as the rule of mixtures. It is introduced to calculate young's modulus and the strength of the composite materials. That is, the rule of mixtures is a calculation method to work out mechanical and physical properties of composites using the matrix and fibre mechanical and physical properties. These calculations are based on an even distribution of fibres within a uniformed matrix. In addition, the matrix is a solid, homogenous alloy with no additional material, as demonstrated in Figure 3. The outer region is where the rule of mixtures is used, and this region is designed starting with radius = 20 mm to outer radius, 30 mm. Having established that meshing in the presence of small hollow spheres generates over 15,000,000 elements in actual hip implant, conventional approach FEA proved to be impossible, and in fact mesh generation failed to operate. Due to this, the only way to conduct this research is to resort to the rule of mixtures.

Composite stiffness can be predicted using a micro-mechanic's approach termed the rule of mixtures. The two main derivation from elastic modulus in rule of mixtures are the upper bound and the lower bound. For this study, upper bound was used and the derivation is demonstrated in detail.

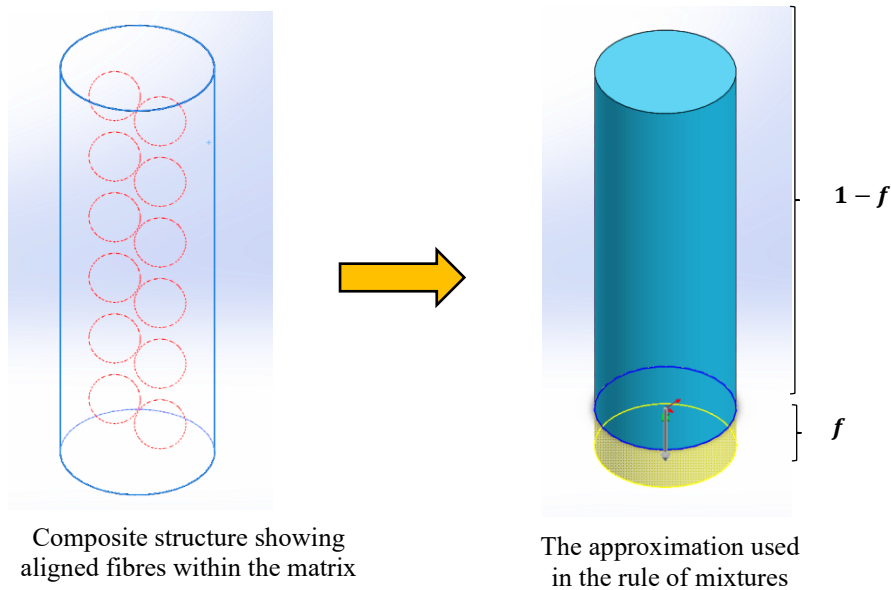


Figure 3: The matrix and fibres in the composite materials

RESULTS AND DISCUSSION

Finite Element Analysis

The results of FEA analysis on samples shows the stiffness of the samples. The displacement of the specimens remains approximately similar between 0.018-0.022 mm due to the similar volume extraction from the solid stainless steel. The specimens containing spheres with 1, 1.5 and 2 mm radius have two different designs each, with the difference being the distance to the side surface of the cylinders to the spheres. Their analysis has elicited that the samples containing spheres closer to the side surface have lower stress compared to those closer to each other. In addition, the size of sphere affects the stress concentration near to it and the larger it is, the lower the stress concentration

close to the surface. However, once the size of sphere reaches 4 mm, the stress concentration remains constant, being also similar to those with a 3 mm and 3.5 mm radius. The stress close to the surface remains approximately similar in all of the hollow sphered samples and the size of spheres also affects the displacement in, i.e. the bigger the size of the sphere is, the higher is the displacement. Therefore, it will result in higher load-transfer onto the bone to decrease the effect of stress shielding. The simulation results show the displacement of samples when a 10 KN force is applied. The Young's modulus of each model has been calculated using their stress and strain. Stress is force divided by the area and strain is displacement over the height.

Table 2: Finite element results for sphered cylinders

<i>Samples</i>	<i>Displacement (mm)</i>	<i>Force applied (N)</i>	<i>E (GPa)</i>
<i>Solid</i>	0.01668	10000	201
<i>R1</i>	0.01997	10000	168
<i>R1.5</i>	0.02053	10000	164
<i>R2</i>	0.02043	10000	164
<i>R3</i>	0.02167	10000	155
<i>R3.5</i>	0.02226	10000	151
<i>R4</i>	0.02265	10000	148

Table demonstrates the results of Young's modulus in FEA. As can be observed, a reduction occurs in this modulus when spheres are included within the volume when compared to the solid model. Furthermore, as the size of spheres increases, the reduction in Young's

modulus is greater. These finite element results also prove that the distance of the spheres from each other and the surface do not make a big difference in the outcome.

COMPRESSION RESULTS

The results obtained from experimental and manual measurements are represented in Table . Table also displays how the mass reductions in the calculated and experimental results are approximately similar and that the samples containing spheres weigh less than the solid one. Furthermore, it is also shown that the UTS_C of the samples containing spheres are approximately similar to each other, that for solid stainless steel being

just slightly higher. However, the reduction is significant in the cylinder containing spheres with 4 mm radius. It can also be observed that the E_C magnitude in the samples containing spheres is smaller compared to the solid one. In addition, E_C in the samples containing spheres is almost similar; however, the reduction in sphere size of radius 4 mm is significant. Furthermore, the compression modulus for the samples pertaining to new designs (two samples) is similar to that of the solid sample.

Table 3: Experimental results for hollow cylinders

Samples	Deduction of sample weight (experiment)	Weight of sample/g (calculation)	UTS_C (MPa)	Deduction of sample E_C (GPa)
R1	34	30.75	453.61	41.05
R1.5	34	30.36	499.78	40.24
R2	34	30.75	506.40	38.98
R3	33	30.36	494.24	39.91
R3.5	34	29.68	448.07	37.93
R4	33.6	29.70	402.76	35.15
Solid	35	33.93	574.30	45.03

RULE OF MIXTURES

Table 4 demonstrates the results of the Young's modulus and strength after calculations based on the rule of mixtures. As it can be observed, the young's modulus of all the samples containing spheres was less than for the solid structure. The volume of cylinders is similar and the extracted volume of each sample is

approximately the same. As Table 4 shows, f is between 0.09-0.12. Furthermore, Table 4 proves that the Young's modulus of all of the sphered cylinders is approximately similar due to the f values. Hence, this shows that the size of spheres and how far they are positioned from each other or the surface do not affect the young's modulus according to the rule of mixtures.

Table 4: Calculation results for different hollow cylinder designs

samples	No of sphere	R_s (mm)	V_{cy} (mm ³)	V_s (mm ³)	f	E (GPa)	Strength (Mpa)
Solid cylinder	0	0	4295.52	0	0	200	1000
R1n96	96	1	4295.52	401.92	0.093567251	181.28	906.43
R1.5n32	32	1.5	4295.52	452.16	0.105263158	178.94	894.73
R2n12	12	2	4295.52	401.92	0.093567251	181.28	906.43
R3	4	3	4295.52	452.16	0.105263158	178.94	894.73
R3.5	3	3.5	4295.52	538.51	0.125365497	174.92	874.63
R4	2	4	4295.52	535.893	0.124756335	175.04	875.24

CONCLUSION

In conclusion, this paper has presented the designs and results for cylinders with hollow spheres being distributed evenly in a controlled mass. Regarding the results, these prove that samples with hollow spheres have a smaller Young's modulus in comparison to solid samples. Experimental results showed that as the radius of hollow spheres increases, the compression modulus for the sphered sample decreases, but titanium compression modulus is still the lowest. The compression modulus for solid titanium is 30 GPa and for solid stainless steel is 45 GPa. However, it is 35 GPa

for sphered samples, which is smaller than solid stainless steel and larger than solid titanium. The FEA results also displayed that the Young's modulus for hollow sphered samples decrease depending on the size of the hollow spheres, the larger the size of hollow spheres, the more the reduction in the Young's modulus is observed. In addition, the Young's modulus for solid titanium is 114 GPa, Solid stainless steel is 200 GPa and hollow sphered sample is 148 GPa. The rule of mixtures displayed similar reduction in all hollow sphered samples Young's modulus, 175 GPa, due to the constant extracted volume from all the samples.

REFERENCES

- [1] T. Thielen, S. Maas, A. Zuerbes, D. Waldmann, K. Anagnostakos, and J. Kelm, "Development of a reinforced PMMA-based hip spacer adapted to patients' needs," *Medical Engineering & Physics*, vol. 31, pp. 930–936, 2009.
- [2] M. Niinomi, "Metallic biomaterials," *J Artif Organs*, vol. 11, no. 3, pp. 105-110, 2008.
- [3] M. Karanjai, R. Sundaresan, G. V. N. Rao, T. R. R. Mohan, and B. P. Kashyap, "Development of titanium based biocomposite by powder metallurgy processing with in situ forming of Ca–P phases," *Materials Science and Engineering: A*, vol. 447, no. 1-2, pp. 19-26, 2007.
- [4] C. Bitsakos, J. Kerner, I. Fisher, and A. A. Amis, "The effect of muscle loading on the simulation of bone remodelling in the proximal femur," *Journal of Biomechanics*, vol. 38, no. 1, pp. 133–139, 2005.
- [5] P. Diegel, A. Daniels, and H. Dunn, "Initial effect of collarless stem stiffness on femoral bone strain," *The Journal of arthroplasty*, vol. 4, no. 2, pp. 173-178, 1989.
- [6] H. E. Jergesen and J. W. Karlen, "Clinical outcome in total hip arthroplasty using a cemented titanium femoral prosthesis," *J. Arthroplasty*, vol. 17, no. 5, pp. 592–599, 2002.
- [7] C. Mattheck, U. Vorberg, and C. Kranz, "Effects of hollow shaft endoprosthesis on stress distribution in cortical bone," *Biomed Tech*, vol. 35, no. 12, pp. 316-319, 1990.
- [8] J. Schmidt and H. Hackenbroch, "The Cenos hollow stem in total hip arthroplasty: first experiences in a prospective study," *Arch Orthop Trauma Surg*, vol. 113, no. 3, pp. 117-120, 1994.
- [9] S. Gross and E. W. Abel, "A finite element analysis of hollow stemmed hip prostheses as a means of reducing stress shielding of the femur," *Journal of Biomechanics*, vol. 34, no. 8, pp. 995-1003, 2001.
- [10] P. Chang *et al.*, "Design and analysis of robust total joint replacements: finite element model experiments with environmental variables," *Journal of Biomechanical Engineering*, vol. 123, pp. 239-246, 2001.
- [11] M. I. Z. Ridzwan, S. Shuib, A. Y. Hassan, A. A. Shokri, and M. N. Mohamad Ibrahim, "Problem of Stress Shielding and Improvement to the Hip Implant Designs: A Review," *Journal of Medical Sciences*, vol. 7, pp. 460-467, 2007.
- [12] M. Sanami, N. Ravirala, K. Alderson, and A. Alderson, "Auxetic materials for sports applications," *ScienceDirect*, vol. 72, pp. 453 – 458, 2014.
- [13] M. Sanami, "AUXETIC MATERIALS FOR BIOMEDICAL APPLICATIONS," University of Bolton, Bolton 2015.
- [14] O. Duncan *et al.*, "Review of auxetic materials for sports applications: Expanding options in comfort and protection," *Applied Sciences*, vol. 8, no. 6, p. 941, 2018.
- [15] C. Moroney, A. Alderson, T. Allen, M. Sanami, and P. Venkatraman, "The application of auxetic material for protective sports apparel," in *Multidisciplinary Digital Publishing Institute Proceedings*, 2018, vol. 2, no. 6, p. 251.
- [16] H. Wang and J. Y. Lim, "Metal-ceramic bond strength of a cobalt chromium alloy for dental prosthetic restorations with a porous structure using metal 3D printing," *Computers in biology and medicine*, vol. 112, p. 103364, 2019.
- [17] J.-H. Lin, C. H. He, M.-C. Lee, Y.-S. Chen, and C.-W. Lou, "Sports protective elastic knits: structure design and property evaluations," *The Journal of The Textile Institute*, vol. 111, no. 3, pp. 424-433, 2020.